Comparison of Various Models for Transient Nozzle Flow Simulations Including Time-Resolved Needle Lift

S. Jollet*, T. Willeke, F. Dinkelacker
Institute of Technical Combustion (ITV), Leibniz University of Hanover, Germany
jollet@itv.uni-hannover.de and dinkelacker@itv.uni-hannover.de

Abstract

Injection systems of modern diesel engines are one of the key components to increase the fuel efficiency and to lower pollutant emissions. Therefore, a detailed understanding of the spray generated by the injector nozzle is crucial to optimize the process of the mixture formation, ignition, combustion, and emission. In diesel injection systems the spray formation is significantly influenced by the internal flow of the injector and often influenced by cavitation. Increasingly important is the transient flow behavior during the needle lift. The aim of this study is the time-dependent numerical simulation of the internal flow processes including the multiphase processes with special emphasis to the time-dependent variation of the needle. The injector consists of a needle with an adapted needle cone geometry and a 8-hole sac-hole nozzle. The holes have a diameter of $d = 247\ \mu m$ with cylindrical geometry and sharp edges at the inlets. Experimental test data from a cold injection chamber provide boundary conditions and serve as a plausibility check. The injector needle movement is realized by a dynamic mesh. Several models have been evaluated. These were the combinations of two multiphase models (Eulerian and Mixture model), two cavitation models (Schnerr-und-Sauer, Zwart-Gerber-Belamri). A suitable combination is found from subsequent studies. Also the influence of vapour pressure was investigated. First results show strongly asymmetric two phase regions inside the nozzle for the transient initial and final part of the injection.

Introduction

Increasing demands in terms of engine performance and fuel consumption as well as even more stringent emissions standards require a continuous development of diesel engines. It is known that the fuel injection has a significant influence on the mixture composition and on the formation of pollutants. To produce typical droplet sizes in the range of 10 μm with fast vaporization and mixing, very high injection pressures up to 2000 bar are established in modern diesel engines, while on the other side the injection duration is decreasing. Both, extremely high pressure and unsteady effects, indicates that the details of the flow and phase change processes inside the injector are of increasing importance for such injectors. The aim of ongoing work is to develop predictive tools for the numerical simulation of these processes. It can be used at the Institute of Technical Combustion on existing knowledge in the numerical treatment of internal nozzle flow and spray break-up [1]. Details of the time-dependent geometry like that of the lifting needle are as important as the two phase processes inside the injector. Here, for instance, cavitation effects can occur. Cavitation effects in the injection port area destabilize the emergent fuel jet and improve the jet break-up [2].

Geometry

Usually diesel injectors (Figure (1)) have several nozzle holes, to distribute the fuel into a large volume of the cylinder. Atomization requires a high injection pressure or a high outlet impulse of the fuel spray. Main parameters of the hole nozzle geometry are the number of nozzle holes, the nozzle hole diameter, the nozzle hole length, and the blind hole volume. It has been found out in the past that additionally details like the curvature on the inflow side of the nozzle hole has a significant influence on the flow of the liquid phase as well as on two phase effects like cavitation behaviour in the nozzle hole.

A major disadvantage of the hole nozzles is the blind hole volume, which remains filled with liquid fuel at the end of injection. This remaining fuel slowly leaks into the combustion chamber and is not burned completely. Accordingly the sac hole volume influences the amount of unburned hydrocarbons in the exhaust.

For the investigated injector an eight hole nozzle (Figure (1)) with a nozzle hole diameter of 247 μm is used. The needle diameter is down to 2,55 mm at a needle tip angle of 95,9°. The sac-hole diameter is down to 1,3 mm and has a needle seat angle of 90°.

*Corresponding author: jollet@itv.uni-hannover.de

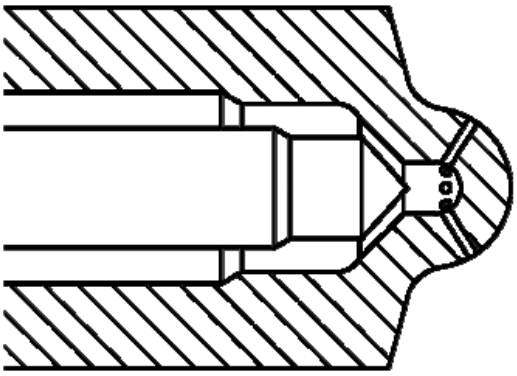

Figure 1. Nozzle geometry of an injector with a sac hole

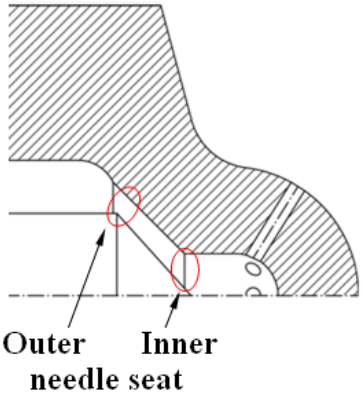

Figure 2. Detail of the injector with the needle seat

Fundamentals

In high pressure injection systems two-phase flow phenomena are known to be important, where for instance the liquid fuel phase and a fuel vapor phase can exist due to cavitation phenomena, and where close to the nozzle exit the liquid fuel phase can be formed in ligaments or droplets being surrounded from a gas phase of the vaporized fuel and of air. For the numerical simulation of multiphase flows, the term "phase" is in sofar generalized as it refers to a flow component that defines flow characteristics and affects the multiphase flow, directly [3]. This definition allows the distinction of phases despite of the same physical appearance and the same material. Many technical multiphase flows can be simplified as a two-phase flow [4].

The numerical simulation of single phase flows is commonly based on methods of computational fluid dynamics (CFD) [5]. For multiphase flows, however, more advanced modelling approaches are necessary.

For this study two multiphase models ared used, the Eulerian two-fluid-model and the mixture model [6].

The "Eulerian" multiphase model belongs to the two-fluid-models. For description of the multiphase conversion of mass a distinction is drawn between a unique and combined phase continuity equation. The unique phase continuity equation will be verbalized for each single phase [6] with the phase density ρ_N, the volume fraction α_N and the single volume flow $j_{N,i}$. The right side of the unique continuity equation is not zero. The mass interaction term I_N discribes the change of the phase mass due to phase transition or chemical reactions [6]. The sum of all unique phase continuity equations defines the combined phase continuity equation (Equation (1)). The right side of the Equation (1) must be zero, so that all mass interaction terms I_N are compensated $\sum_N I_N = 0$:

$$\frac{\partial}{\partial t}\left[\sum_N (\rho_N \alpha_N)\right] + \frac{\partial}{\partial x_i}\left[\sum_N (\rho_N j_{N,i})\right] = \sum_N I_N = 0. \tag{1}$$

Accordingly the individual and the combined momentum equations (Equation (2), with the Einstein notation stating that a summation over all spatial coordinate directions is done if the same index appears twice in one summand with the velocity $u_{N,k}$,$u_{N,i}$, the gravity g_k, the pressure p and the the deviatoric stress tensor σ^D_{Cki}) can be written as [6]

$$\frac{\partial}{\partial t}\left[\sum_N (\rho_N \alpha_N u_{N,k})\right] + \frac{\partial}{\partial x_i}\left[\sum_N (\rho_N \alpha_N u_{N,i} u_{N,k})\right] = \rho_N g_k - \frac{\partial p}{\partial x_k} + \frac{\partial \sigma^D_{Cki}}{\partial x_i}. \tag{2}$$

Also the multiphase energy conservation equation consists of the individual and the combined energy equation. The specific energy $e^*_N = e_N + e_{kin,N} + e_{pot,N}$ includes the inner energy e_N, the kinetic energy $e_{kin,N}$ and the elevation energy $e_{pot,N}$ of the phase N. The combined phase energy equation (Equation (3)) is derived from the sum of the single energy equations and of the summary of the external terms $q = \sum_N q_N$ and $w = \sum_N w_N$ with

the the continuous phase stress tensor σ_{Cij} and the velocity u_{Ni}:

$$\frac{\partial}{\partial t}\left[\sum_N \left(\rho_N \alpha_N e_N^*\right)\right] + \frac{\partial}{\partial x_i}\left[-u_{Ci}\sigma_{Cij}\sum_N \left(\rho_N \alpha_N e_N^* u_{Ni}\right)\right] = q + w. \tag{3}$$

The so-called "Mixture model" describes the multiphase flow by a mixing formulation. Instead of individual phase conversion equations like in the case of the "Eulerian model" the conversion equation is described for the total mixture. In the combined continuity equation (Equation (1)) the phase volumen flow j_{Ni} will be replaced:

$$\frac{\partial}{\partial t}\left[\sum_N \left(\rho_N \alpha_N\right)\right] + \frac{\partial}{\partial x_i}\left[\sum_N \left(\rho_N \alpha_N u_{Ni}\right)\right] = 0. \tag{4}$$

Applying the mixture density $\rho_{mix} = \sum_N \alpha_N \rho_N$, the velocity $u_{i,mix} = \sum_N \left(\left(\alpha_N \rho_N u_{i,N}\right)/\rho_{mix}\right)$ and the equation (4), the mixture continuity equation (5) is defined as

$$\frac{\partial}{\partial t}\left(\rho_{mix}\right) + \frac{\partial}{\partial x_i}\left(\rho_{mix} u_i\right) = 0. \tag{5}$$

The same approach leads to the mixture momentum equations (Equation (6)) with the additional body force k_i, the mixture viscosity η_{mix} and the drift velocity $u_{i,dr,N} = u_{i,N} - u_{i,mix}$ between the mixture and the phase N:

$$\begin{aligned} \tfrac{\partial}{\partial t}\left(\rho_{mix} u_{i,mix}\right) + \tfrac{\partial}{\partial x_i}\left(\rho_{mix} u_{i,mix} u_{j,mix}\right) &= \rho_{mix} k_i - \tfrac{\partial p}{\partial x_i} \\ &\quad + \tfrac{\partial}{\partial x_j}\left[\eta_{mix}\left(\tfrac{\partial u_{i,mix}}{\partial x_j} + \tfrac{\partial u_{j,mix}}{\partial x_i}\right)\right] \\ &\quad + \tfrac{\partial}{\partial x_j}\left[\textstyle\sum_N \left(\alpha_N \rho_N u_{i,dr,N} u_{j,dr,N}\right)\right]. \end{aligned} \tag{6}$$

The mixture energy equation (7) is calculated as follows [6]

$$\frac{\partial}{\partial t}\left[\sum_N \left(\rho_N \alpha_N e_N\right)\right] + \frac{\partial}{\partial x_i}\left[\sum_N \left(\alpha_N u_{i,N}\left(\rho_N e_N + p\right)\right)\right] = \frac{\partial}{\partial x_i}\left(k_{eff}\frac{\partial T}{\partial x_i}\right) + S_e \tag{7}$$

with the effektive conductivity k_{eff}, the temperature T and volumetric heat sources S_e.

The expression "cavitation" designates the change of the phase from the liquid to the vapour phase because of a strong pressure drop. For the formation of a cavitation bubble, the liquid pressure p must locally fall below the vapour pressure p_v. Cavitation modelling is commonly based on the Rayleigh-Plesset-Equation (8). This equation describes the pressure-dependent dynamics of the growth of bubbles with radius R_B in a compressible fluid:

$$R_B \ddot{R}_B + \frac{3}{2}\dot{R}_B^2 = \frac{1}{\rho_l}\left[p_v - p_h - \frac{2\sigma}{R_B} - 4\eta_l \frac{\dot{R}_B}{R_B}\right]. \tag{8}$$

with first and second derivation of the radius, with the density of the liquid ρ_l, the surface tension σ and the viscosity of the liquid η_l.

Simplifying equation (8) the second time derivation $\ddot{R}_B$, the surface tension and the viscosity of the liquid is neglected. Then the growing or contracting rate of the bubble is essentially a function of the difference between the internal bubble pressure p_v and the hydrostatic liquid pressure $p_h = p_0 + \rho_l g h$ (with the ambient pressure p_0 and the pressure at the height h):

$$\dot{R}_B = \sqrt{\frac{2}{3}\frac{\left(p_v - p_h\right)}{\rho_l}}. \tag{9}$$

For the application in two-phase models essentially the mass transfer rate R between the liquid and the gas phase is needed. Two models are compared, both being based on the simplified Rayleigh-Plesset-Equation.

The Schnerr-und-Sauer cavitation modell [7] describes the mass transfer rate being proportional to a volume change rate $\dot{\alpha_v}$, the densities of the vapour ρ_v and of the liquid phase ρ_l, and of the mixture ρ_{mix} with

$$R = \frac{\rho_v \cdot \rho_l}{\rho_{mix}} \cdot \dot{\alpha}_v. \tag{10}$$

The steam quantity $\alpha_v = (n_B(4)/(3)\pi R_B^3)/(1 + n_B(4)/(3)\pi R_B^3)$ is a measure the number of steam bubbles n_B. For simplification spherical bubbles are assumed. For the bubble radius R_B follows the relation

$$R_B = \sqrt[3]{\frac{1}{n_B}\frac{3}{4\pi}\frac{\alpha_v}{1-\alpha_v}}. \tag{11}$$

Substitution of these equations and the simplified Rayleigh-Plesset-Equation (9) leads to the transfer coefficients for the cavitation R_e ((Equation (12)) if $p_h \leq p_v$) or the condensation R_c ((Equation (12)) if $p_h \geq p_v$) according to the Schnerr-und-Sauer cavitation model

$$R_i = \frac{3\alpha_v\,(1-\alpha_v)}{R_B}\frac{\rho_v\rho_l}{\rho}\sqrt{\frac{2}{3}\frac{p_v - p_h}{\rho_l}}. \tag{12}$$

The Zwart-Gerber-Belamri cavitation model assumes large vapour bubbles of equal size, which do not affect each other [8]. The netto mass exchange coefficient R is based on the bulk change of one unit vapour bubble, where the decrement and the absorbed vapour mass is computed by the number of bubbles n_B, the bubble surface, the vapour density and the change of the radius $\dot{R}_B$:

$$R = n_B 4\pi R_B^2 \dot{R}_B \rho_v. \tag{13}$$

Additionally the vapour fraction $\alpha_v = n_B 4/3\pi R_B^2$ will be calculated by the number of bubbles n_B and the volume of the bubbles. The onset of α_v into the equation (13) is due to connection between the transfer rate R and the change rate of the radius $\dot{R}_B$:

$$R = 3\alpha_v\rho_v\frac{\dot{R}_B}{R_B}. \tag{14}$$

Equation (14) combined with the simplified Rayleigh-Plesset-Equation (9) forms the mass exchange term R:

$$R = \frac{3\alpha_v\rho_v}{R_B}\sqrt{\frac{2}{3}\frac{(p_v - p_h)}{\rho_l}}. \tag{15}$$

For the evaporation caused by cavitation the vapour fraction α_v will be replaced by $\alpha_{nuc}\,(1-\alpha_v)$. The α_{nuc} term describes the density of the nuclei, where vapour bubbles can arise. The term $\alpha_{nuc}\,(1-\alpha_v)$ describes the progression of the nucleus, that deactivates due to increasing vapour fraction. Introducing an evaporation coefficient F_{vap} and a condensation coefficient F_{cond} the transfer rates for cavitation R_e or condensation R_c are given for the Zwart-Gerber-Belamri cavitation model with

$$R_e = F_{vap}\frac{3\alpha_{nuc}\,(1-\alpha_v)\,\rho_v}{R_B}\sqrt{\frac{2}{3}\frac{p_v - p_h}{\rho_l}} \qquad if\ p_h \leq p_v, \tag{16}$$

$$R_c = F_{cond}\frac{3\alpha_{nuc}\rho_v}{R_B}\sqrt{\frac{2}{3}\frac{p_v - p_h}{\rho_l}} \qquad if\ p_h \geq p_v. \tag{17}$$

Results and Discussion

In a first study the sensitivity of the simulation approach is examined for the aspects of the numerical mesh resolution, the turbulence model, as well as for the multiphase and the cavitation model and of the vapour pressure. For this reason time-independent simulations of the internal injection flow have been done.

In a mesh study the influence of the spatial discretization effects are examined. For two needle positions (0.3 mm and 0.0668 mm) the flow has been calculated with different fine resolved grids. The geometry corresponds to half of an injector with three full and two half spray holes with a plane symmetry. A hybrid mesh of hexahedral and tetrahedral elements has been used. The flow is simulated as a single phase, incompressible and frictionless flow, so that the maximum flow velocity is achieved. The inlet boundary conditions were selected with $p_{in} = 1400\ bar$ and 60 °C for pressure and temperature, for the outlet $p_{out} = 29\ bar$ and 28 °C was used. The wall interaction was set to adiabatic. Diesel (liquid) was assumed as a single phase medium.

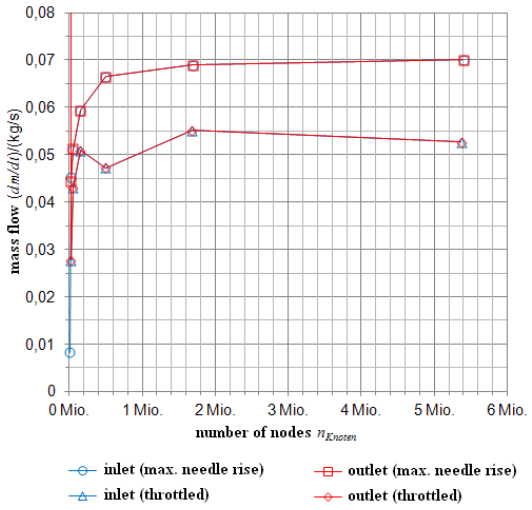

Figure 3. Mesh study

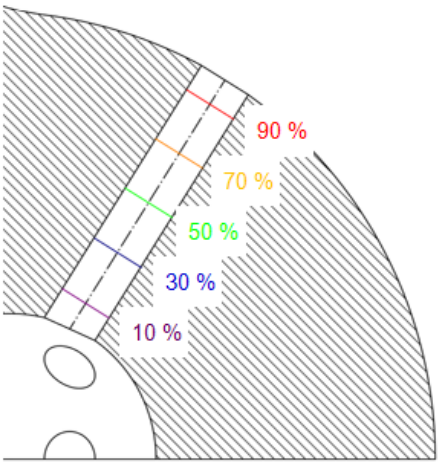

Figure 4. Profiles at the positions x/L

For the mesh study the mass flow rates through the inlet and the outlet are calculated for numerical grids with different number of nodes. The Figure 3 shows that the grid independency is reached at a number of about 1.6 million nodes.

A sensitivity analysis of the required boundary layer resolution for the y^+ values and the mass flow result shows that at least 20 prism layers are required in the near-wall area. For a turbulence modelling study three turbulence models (k-ε, k-ω and SST (Shear Stress Transport)) and two boundary layer models (WF (Wall Function) and EWT (Enhanced Wall Treatment)) have been applied. In addition, the prism varied the link between the boundary layer region and the flow region.

The WF boundary layer model is found to be out of its range of application in these small scale structures, as the boundary layer is not sufficiently resolved for the turbulence-model-specific dimensionless wall distance y^+. Therefore the EWT wall function approach is used in the following.

Tests have been made to compare the calculated mass flow rates with those being determined experimentally. It is found that all predictions show 6 to 10% lower rates than the experiment (k-ε-model and k-ω-model 9-10%, SST-model 6%). Comparing flow rates at different positions in the spray hole, the SST-model shows large mass flow inequalities, being sensitive to the wall resolutions, while the k-ε- and k-ω-model with EWT formulation satisfy the continuity conditions. Additionally the SST-model shows an inconclusive behaviour for the velocity profiles in the transition between the boundary layer region and the inner flow region. As a conclusion the standard-k-ε-turbulence model with EWT-formulation is used in the following.

As the next step multi-phase simulations have been carried out. Here two multi-phase models (Eulerian and Mixture-model) are combined with two cavitation models (Schnerr-Sauer and Zwart-Gerber-Belamri model). The liquid diesel fuel is taken as the carrier phase while gaseous diesel vapour is the disperse phase. As the phase

transition depends on the vapour pressure, which by itself is strongly temperature dependent, a study (Figure 11) has been performed with vapour pressures between 100 and 3000 Pa (corresponding to temperatures between 20 and 60 °C [9][10][11].

In the Figures (5)-(8) the influence of the model approaches on the phase change predictions is shown. The influence of the multiphase model is significant while the influence of the cavitation modell is rather small. With each of these model configurations a significantly asymmetric distribution of the vapour phase has been calculated. Profiles of the vapour phase show the development inside the injection holes (Figure (9) and (10)). The multiphase models lead to different predictions.

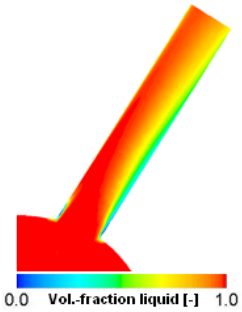

Figure 5. Eulerian model with the Schnerr-und-Sauer cavitation model

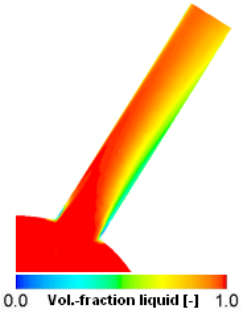

Figure 6. Eulerian model with the Zwart-Gerber-Belamri cavitation model

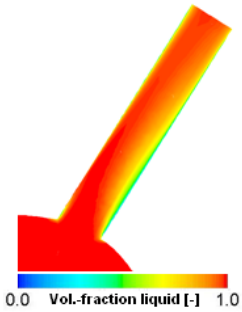

Figure 7. Mixture model with the Schnerr-und-Sauer cavitation model

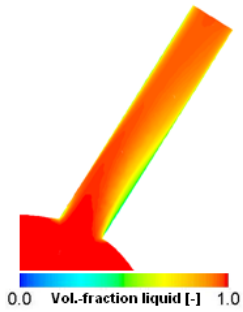

Figure 8. Mixture model with the Zwart-Gerber-Belamri cavitation model

Which of the two multiphase models is nearer to the reality is not yet known, however, the simulation studies give clear indications that also experimental work should be done with the inclusion of the time-dependent processes [12] in order to allow more accurate comparison for the model development.

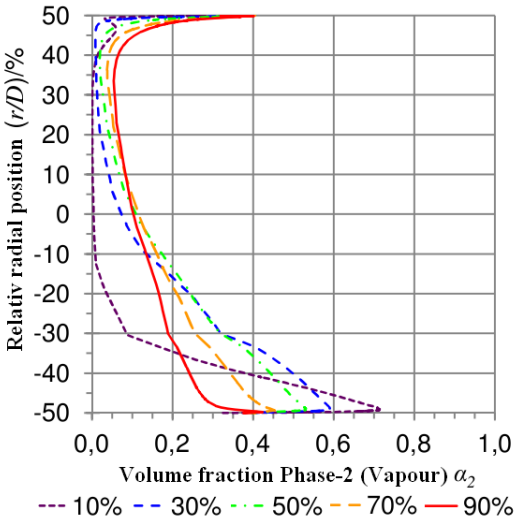

Figure 9. Volume fraction of the vapour phase in different profiles (Figure 4) in the injection hole. Eulerian model with the Zwart-Gerber-Belamri cavitation model.

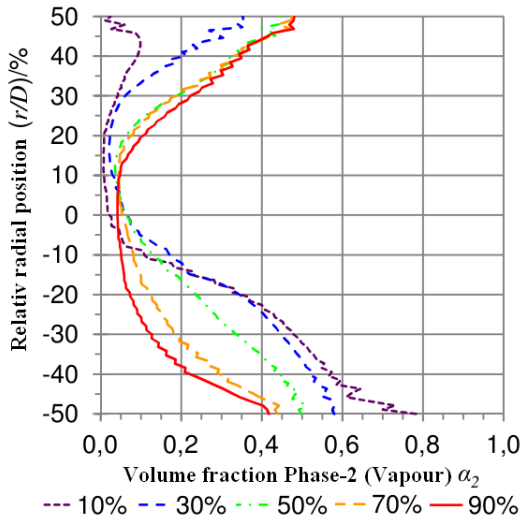

Figure 10. Volume fraction of the vapour phase in different profiles (Figure 4) in the injection hole. Mixture model with the Zwart-Gerber-Belamri cavitation model.

Figure (11) shows for steady flow simulations that the influence of the two-phase and cavitation models on the predicted amount of vapour coming through the exit plane of the nozzle hole is significant, while the vapour pressure has no influence.

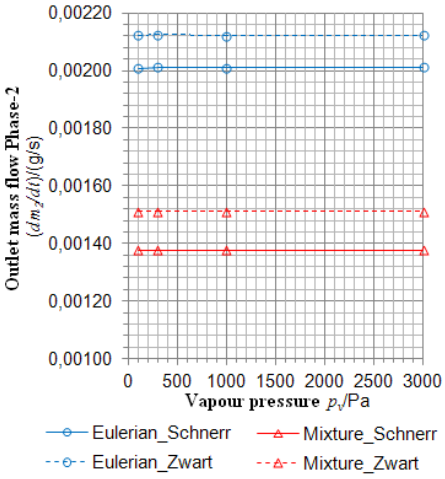

Figure 11. Vapour pressure depend of the vapour mass flow

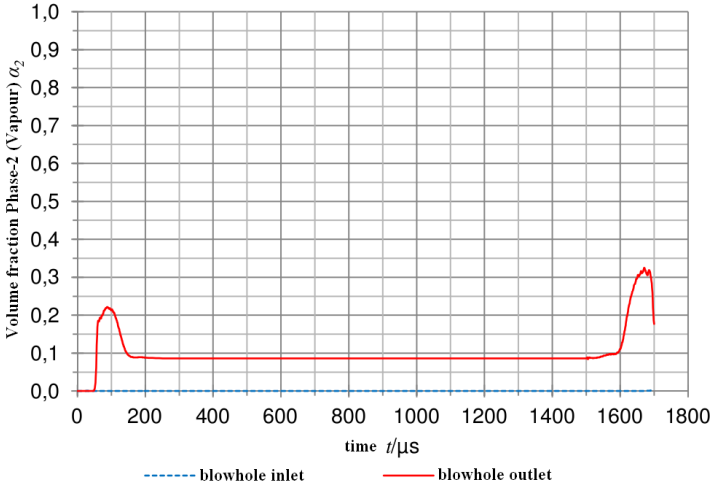

Figure 12. Volume fraction development of the vapour into the blowhole (Mixture multiphase model and Zwart-Gerber-Belamri cavitation model)

In a final study dynamic transient calculations have been made, where the needle has an injection period of 1700 μs. Included in the injection period is the opening and the closing time of 200 μs. For this calculation, the same pressure and temperature boundary conditions were used as for the stationary investigations. Based on the sensitivity analysis with stationary simulations, the full dynamic transient simulation have been done with the standard-k-ε-turbulence model with EWT-formulation, the mixture multiphase model and Zwart-Gerber-Belamri cavitation model. According to its negligible influence, the vapour pressure is set to a preheated diesel fuel temperature of 60 °C and 3000 Pa.

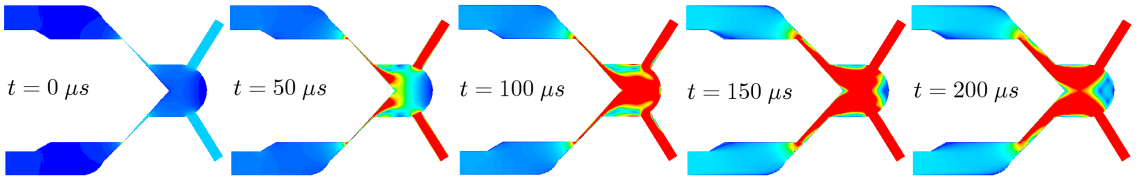

Figure 13. Opening process of the transient dynamic injection flow

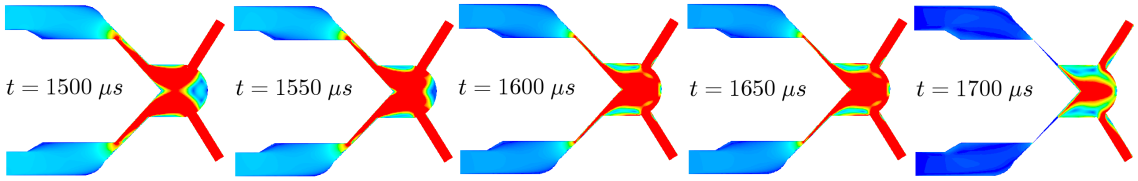

Figure 14. Closing process of the transient dynamic injection flow

Interesting is the development of the flow pattern during the opening process of the needle (Figure (13)). Here the velocity is shown color-coded. The influence of details of geometry between needle and needle seat is clearly visible, as here the momentum wave of the fluid is starting. In the third image ($t = 100\ \mu s$) this wave has reached the end of the sac-hole, leading to strongly inhomogeneous inflow conditions of the spray holes. Later ($t = 200\ \mu s$) more constant flow conditions are reached with less curved flow paths. This inhomogeneous transient flow conditions have a strong impact on the two-phase processes inside the spray holes. It is clearly visible that

the mentioned transient inhomogeneous inflow leads to strongly asymmetric flow conditions inside the injector holes. The closing process of the needle shows partly a reverse behaviour. Again the flow field at the entrance of the injection holes turnes to be unsymmetric and the simulation predicts the corresponding increased amount of vapour content. This transient inflow simulations indicate that also the spray behaviour behind the injector should be expected to be unsymmetric. Corresponding time resolved experiments are planned. The Figure (12) shows an example of the time-dependent volume fraction of the vapour phase. It can be noted that the moving of the needle caused an increase of the volume fraction of vapour during the opening and closing period.

Summary and Conclusions

In this work, the flow within a diesel injector is simulated numerically. The geometrical details of the injector with its sac-hole and of the movable nozzle needle have been regarded. All eight injection holes are cylindrical holes with sharp inlet edges. Experiments of the same injector done in a high pressure test cell serve as a reference and for testing the plausibility of the simulation results. Aim of this work is the evaluation of suitable submodels for the dynamic unsteady simulation of the physical processes inside the diesel injector including a movable injector. The required grid resolution and suitable turbulence, multiphase and cavitation models are analysed separately. In addition, the vapour pressure influence is examined.

Subsequent studies of combinations of two multiphase models (Eulerian, Mixture) and two cavitation models (Schnerr-and-Sauer, Zwart-Gerber-Belamri) and the application of four different vapour pressures clearly show the influences of the multiphase model. Differences between the two investigated cavitation models are found to be small and effects of different vapour pressure values are negligible.

In the following part of the study unsteady simulations have been made with the two-phase mixture model and the Zwart-Gerber-Belamri cavitation model, considering the complete injection process. The unsteady processes strongly depend on the geometrical details of the lifting needle and the needle seat as well as on the geometry of the sac hole. For the given geometry a momentum wave is observed leading to strongly unsymmetrical flow conditions during the initial stage of the lifting needle. This inhomogeneous transient flow conditions have a strong impact on the two-phase processes inside the spray holes, showing a strong unsymmetric distribution of the cavitation region with high vapour content, especially in the transient initial and final steps of ignition.

References

[1] Baumgarten, C., Merker, G.P., *Modellierung des Primärzerfalls bei der Hochdruck-Dieseleinspritzung*, MTZ Artikel 4/2004 Jahrgang 65, ITV Hannover, 2004.

[2] Walther, J., *Quantitative Untersuchung der Innenströmung in kavitierenden Dieseleinspritzdüsen*, Dissertation, TU Darmstadt, 2002.

[3] ANSYS, Inc., *ANSYS FLUENT Theory Guide*, *Release 13.0* ANSYS, Ic., (2010)

[4] Yeoh, G. H., Tu, J. *Computational Techniques for Multi-Phase Flows - Basics and Applications*, 1st Edition, Butterworth-Heinemann, 2010.

[5] Patankar, S.V., *Numerical Heat Transfer and Fluid Flow*, McGraw-Hill, 1980.

[6] Brennen, C. E., *Fundamentals of Multiphase Flow*, Paperback Edition, Camebridge University Press, 2009.

[7] Schnerr, G.H., Sauer, J. *Physical and Numerical Modeling of Unsteady Cavitation Dynamics*, In Fourth International Conference on Multiphase Flow, New Orleans, USA, 2001.

[8] Zwart, P.J., Gerber, A.G., Belamri, T. *A Two-Phase Flow Model for Predicting Cavitation Dynamics*, In Fifth International Conference on Multiphase Flow, Yokohama, Japan, 2004.

[9] Eni Deutschland, *EU-Sicherheitsdatenblatt für Dieselkraftstoff*, *http://www.enideutschland.com*, (22.06.2011)

[10] OMV Refining & Marketing GmbH, *Sicherheitsdatenblatt für Dieselkraftstoff*, *http://ehsweb.omv.com*, (22.06.2011)

[11] Wenck, H., Schneider, C., *Chemisch-physikalische Daten von Otto- und Dieselkraftstoffen: DGMK-Projekt 409*, DGMK-Berichte, 1993.

[12] Heilig, A., Kaiser, M., Dinkelacker, F. *Near Nozzle High-Speed Measurements of the Intact Core for Diesel Sprays*, ICLASS, Heidelberg, 2012.